Published in final edited form as:
Eur J Neurosci. 2012 August ; 36(4): 2452–2460. doi:10.1111/j.1460-9568.2012.08170.x.

Postnatal Experience Modulates Functional Properties of Mouse Olfactory Sensory Neurons

Jiwei He, **Huikai Tian**, **Anderson C. Lee**[§], and **Minghong Ma**[*]
Department of Neuroscience, University of Pennsylvania School of Medicine, Philadelphia, PA 19104, USA

Abstract

Early experience considerably modulates the organization and function of all sensory systems. In the mammalian olfactory system, deprivation of the sensory inputs via neonatal, unilateral naris closure has been shown to induce structural, molecular, and functional changes from the olfactory epithelium to the olfactory bulb and cortex. However, it remains unknown how early experience shapes functional properties of individual olfactory sensory neurons (OSNs), the primary odor detectors in the nose. To address this question, we examined odorant response properties of mouse OSNs in both the closed and open nostril after four weeks of unilateral naris closure with age-matched untreated animals as control. Using patch-clamp technique on genetically-tagged OSNs with defined odorant receptors (ORs), we found that sensory deprivation increased the sensitivity of MOR23 neurons in the closed side while overexposure caused the opposite effect in the open side. We next analyzed the response properties including rise time, decay time, and adaptation induced by repeated stimulation in MOR23 and M71 neurons. Even though these two types of neurons showed distinct properties in dynamic range and response kinetics, sensory deprivation significantly slowed down the decay phase of odorant-induced transduction events in both types. Using western blotting and antibody staining, we confirmed upregulation of several signaling proteins in the closed side as compared with the open side. This study suggests that early experience modulates functional properties of OSNs, probably via modifying the signal transduction cascade.

Keywords

naris-closure; experience-dependent plasticity; olfactory signal transduction; patch clamp; and gene-targeting

Introduction

Smell perception in mammals starts with the binding of odorants to specific odorant receptors (ORs) located in the cilia of olfactory sensory neurons (OSNs) in the main olfactory epithelium (MOE). The mouse MOE harbors a few million OSNs and expresses ~1200 G protein-coupled ORs (Zhang et al., 2007). Each OSN expresses a single OR type, which defines its response profile and its central target in the main olfactory bulb (MOB) (Mombaerts, 2006). Binding of odor molecules to ORs leads to increased intracellular cAMP levels via sequential activation of olfactory G protein (Golf) and type III adenylyl

[*]**Correspondence to**: Dr. Minghong Ma, Department of Neuroscience, University of Pennsylvania School of Medicine, 215 Stemmler Hall, 3450 Hamilton Walk, Philadelphia, PA 19104, USA. Tel: +1 (215) 746-2790; Fax: +1 (215) 573-9050; minghong@mail.med.upenn.edu..
[§]Current address: Department of Biochemistry and Molecular Biophysics and Howard Hughes Medical Institute, Columbia University, New York, NY 10032, USA

cyclase (ACIII). Subsequent opening of a cyclic nucleotide-gated (CNG) channel and a Ca^{2+}-activated Cl^- channel depolarizes OSNs, which fire action potentials that transmit odor information to the MOB (Su *et al.*, 2009; Touhara & Vosshall, 2009). This odorant-activated cAMP cascade, like all other G-protein mediated signal transduction pathways, is subject to negative feedback at every major step, which contributes to response termination (or deactivation) and adaptation (Zufall & Leinders-Zufall, 2000; Ma, 2007).

Experience plays critical roles in development of smell perception by fine-tuning the neural circuitry because this system undergoes considerable growth and neurogenesis postnatally. Unilateral naris closure is a procedure widely used in investigating the effects of sensory inputs on the organization and function of the rodent olfactory system. The closed side is deprived of most airflow and odorant influx, while the open side, acting as the obligatory breather, carries increased airflow and odorant influx. This procedure has been shown to cause structural, molecular, and functional changes in the MOE (Benson *et al.*, 1984; Farbman *et al.*, 1988; Cummings & Brunjes, 1994; Coppola *et al.*, 2006; Suh *et al.*, 2006; Waggener & Coppola, 2007; Bennett *et al.*, 2010; Coppola & Waggener, 2012), MOB (Brunjes, 1985; Kosaka *et al.*, 1987; Gomez-Pinilla *et al.*, 1989; Philpot *et al.*, 1997; Liu *et al.*, 1999; Hamilton & Coppola, 2003; Zou *et al.*, 2004; Cummings & Belluscio, 2010), and olfactory cortex (Franks & Isaacson, 2005; Kim *et al.*, 2006). Specifically in the MOE, the closed side showed increased amplitude and slower kinetics in odorant-induced electroolfactogram (EOG) signals as compared with the open side (Waggener & Coppola, 2007). However, because EOG signals summate activities of many OSNs with different OR types and unilateral naris closure alters OR gene expression in both the closed and open side (Coppola & Waggener, 2012), it is essential to measure odorant-induced responses in single cells with defined ORs in order to understand how early experience shapes the function of OSNs.

Here we address this question by comparing odorant response properties of genetically-tagged OSNs with defined ORs (Bozza et al., 2002; Vassalli et al., 2002; Grosmaitre et al., 2006) in the closed and open nostril after four weeks of unilateral naris closure with age-matched untreated mice as control. The results revealed that sensory deprivation increased the sensitivity of MOR23 neurons in the closed side while overexposure caused the opposite effect in the open side. Additionally, sensory deprivation altered the response kinetics by slowing down the decay phase of odorant-induced transduction currents in both MOR23 and M71 neurons. Moreover, there was an upregulation of several signaling proteins in the closed side, mostly in agreement with previous reports (Waguespack *et al.*, 2005; Coppola *et al.*, 2006; Coppola & Waggener, 2012). This study suggests that via modifying the signal transduction cascade, sensory inputs can modulate the functional properties of OSNs.

Materials and Methods

Animals and nasal tissues

Genetically targeted MOR23- or M71-IRES (internal ribosome entry site)-tauGFP mice were used for recording OSNs which coexpress a defined odorant receptor and green fluorescent protein (Bozza et al., 2002; Vassalli et al., 2002). All mice were in a mixed 129 and C57BL/6 genetic background and the breeding pairs were kindly provided by Dr. Peter Mombaerts. For unilateral naris closure, a brief cauterization (<1 s) using a cauterizer (Fine Science Tools) was performed on one nostril at postnatal day 3 (P3) and the animals (either sex) were examined four weeks (± two days) later. Only animals with a complete closure on the operated side were used for further analysis with age-matched untreated mice as control.

Mice were deeply anesthetized by intraperitoneal injection of ketamine (200 mg/kg), and then decapitated. For patch clamp (Ma et al., 1999; Grosmaitre et al., 2006), the head was

immediately put into icy Ringer's solution, which contained (in mM): NaCl 124, KCl 3, $MgSO_4$ 1.3, $CaCl_2$ 2, $NaHCO_3$ 26, NaH_2PO_4 1.25, glucose 15; pH 7.6 and 305 mOsm. The pH was kept at 7.4 after bubbling with 95% O_2 and 5% CO_2. From each nostril, the olfactory mucosa attached to the nasal septum and from the dorsal recess was removed *en bloc* and kept in oxygenated Ringer. Before use, the entire mucosa was peeled away from the underlying bone and transferred to a recording chamber with the mucus layer facing up. While recording, oxygenated Ringer was continuously perfused at 25 ± 2°C. For western blot (Lee *et al.*, 2011), the olfactory mucosa from each nostril was collected in icy Ringer's solution as described above. For immunohistochemistry (Ma *et al.*, 2003; Tian & Ma, 2008), the head was immediately put into 4% paraformaldehyde (Sigma) overnight at 4 °C, and then subject to decalcification in 0.5 M EDTA (pH 8.0, ethylenediaminetetraacetic acid) for two days. The nose was cut into 20 μm coronal sections on a cryostat. The procedures of animal handling and tissue harvesting were approved by the Institutional Animal Care and Use Committee of the University of Pennsylvania.

Patch clamp

The dendritic knobs of OSNs in intact olfactory epithelia were visualized through an upright microscope (Olympus BX61WI) with a 40× water-immersion objective. An extra 4× magnification was achieved by an accessory lens in the light path. The GFP-tagged cells were visualized under fluorescent illumination. Superimposition of the fluorescent and bright field images allowed identification of the fluorescent cells under bright field, which directed the recording pipettes. Electrophysiological recordings were controlled by an EPC-9 amplifier combined with Pulse software (HEKA Electronic, Germany). Perforated patch-clamp was performed on the dendritic knobs by including 260 μM nystatin in the recording pipette, which was filled with the following solution (in mM): KCl 70, KOH 53, methanesulfonic acid 30, EGTA 5.0, HEPES 10, sucrose 70; pH 7.2 (KOH) and 310 mOsm. Under voltage-clamp mode, the signals were initially filtered at 10 kHz and then at 2.9 kHz. For odorant-induced transduction currents, which are relatively slow and long lasting, the signals were sampled at 333 Hz. Further filtering offline at 60 Hz did not change the response kinetics or amplitudes, indicating that the sampling rate was sufficient and that signal aliasing was not a concern.

A seven-barrel pipette, placed ~25 μm downstream from the recording site, was used to deliver stimuli by pressure ejection (at 20 psi or 138 kPa) via a picospritzer (Pressure System IIe). The pulse length was kept at 300 ms to ensure that the neurons were stimulated by the intra-pipette concentration (Grosmaitre et al., 2006) and one barrel was filled with Ringer's to serve as a control for the potential mechanical response (Grosmaitre et al., 2007). Odorants were prepared fresh daily from a concentrated stock at 0.5 M by adding Ringer's. Acetophenone (Cat# A10701; CAS#: 98-86-2) was purchased from Sigma-Aldrich and lyral (CAS#: 31906-04-4) was provided as a generous gift from International Fragrances and Flavors Inc. (New York, NY).

Western blotting

Seven unilateral naris-closed mice at the age of four weeks were used for these experiments. The olfactory mucosa from each nostril was dissected out, transferred to 50 μl SDS solution (containing 1% sodium dodecyl sulfate, 50 mM NaF, and 1 mM EDTA), and then sonicated for 30 seconds. After centrifugation at 16,000 rpm for 3 min under 4 °C, 50 μl supernatant was taken out and mixed with 200 μl buffer containing 20 mM TrisCl pH8.0, 150 mM NaCl, 5 mM EDTA, 1% TritonX100, 10 mM NaF, 2.5 mM Na_3VO_4, 10 mM $Na_4P_2O_7$, 1 μM Leupeptin, 1μM Pepstatin A, and 1μM Aprotinin. Protein concentration was determined by Bradford Assay (Bio-Rad), with bovine serum albumin as standard. Proteins were separated on 8% SDS—polyacrylamide gels and transferred to Hybond-C

nitrocellulose membranes (Amersham Biosciences, UK). Non-specific binding sites were blocked with 5% dry non-fat milk (Carnation) in TBST (10 mM Tris—HCl, pH 8.0, 150 mM NaCl and 0.4% Tween 20) for 1 h at room temperature. The blots were incubated with the same primary antibodies used in immunohistochemistry for 1 h at room temperature or overnight at 4 °C. Blots were washed three times with TBST and then incubated with horseradish peroxidase (HRP)-conjugated secondary antibody for 1 h at room temperature. The primary antibodies included rabbit anti-olfactory marker protein (OMP, 1:100; Santa Cruz, sc-67219), rabbit anti-ACIII (1:200; Santa Cruz, sc-588), rabbit anti-Golf (1:200; Santa Cruz, sc-385), rabbit anti-phosphodiesterase 4A (PDE4A, 1:300; Abcam, ab14607), rabbit anti-phosphodiesterase 1C (PDE1C, 1:300; Abcam, ab14602), mouse anti-β-arrestin-2 (1:200; Santa Cruz Biotechnology, sc-13140), mouse anti-calmodulin (1: 200; Abcam, ab5494), rabbit anti-CNGA2 (CNGA2, 1:200; Chemicon, ab5810), and monoclonal mouse anti-β-actin (1:50,000; Sigma, A5441). The secondary antibodies were HRP-conjugated anti-rabbit antibody (1:1000; Upstate) or HRP-conjugated anti-mouse antibody (1:2000; Upstate). Blots were washed twice with TBST and once with TBS (10 mM Tris—HCl, pH 8.0, 150 mM NaCl). The ECL (Pierce) was used to visualize bound antibodies. Blots were then quantified using the CCD-based FujiFilm (Tokyo, Japan) LAS 3000 system.

Immunohistochemistry

After antigen retrieval in 95 °C waterbath for 12 min, nose sections were first blocked for 60 min in TPBS (0.3% Triton X-100 in phosphate buffered saline) with 2% bovine serum albumin and then incubated at 4 °C with the primary antibodies in the same solution for over night. Immunofluorescence was achieved by reaction with appropriate secondary antibodies at 1:400 for 1 hr. Tissues were washed in TPBS and mounted in Vectashield (Vector Laboratories). Pictures were taken under a Zeiss LSM 510 confocal microscope. In addition to the primary antibodies described in ***Western blotting***, we also used rabbit anti-olfactory marker protein (OMP, 1:100; Santa Cruz, sc-67219) and mouse anti-neural cell adhesion molecule (NCAM, 1:200; Sigma). The secondary antibodies included donkey-anti-mouse-488, donkey-anti-rabbit-568, and donkey-anti-rabbit-488 (Jackson ImmunoResearch Laboratories).

Statistical Analysis

Two-way ANOVA tests for each parameter of odorant responses were performed using the R program. Paired *t* test was performed using the built-in function in Excel. Dose response curves were fit using the GraphPad Prism Software. An average is shown as mean ± standard errors unless otherwise stated.

Results

Sensory experience modulates response properties of MOR23 neurons

To test the effects of sensory inputs on the functional properties of OSNs, we performed unilateral naris closure on P3 mice and measured odorant responses in individual neurons from the closed and open side four weeks later. Age-matched untreated mice were used as control. To facilitate comparison under different conditions, we used a previously-characterized, gene-targeted mouse line in which MOR23 expressing OSNs coexpress GFP (Vassalli et al., 2002; Grosmaitre et al., 2006). Under voltage clamp mode, brief lyral pulses elicited inward currents which can be characterized by various parameters including the rise time, decay time, residual current, and peak currents (Fig. 1A).

We first examined whether the amount of sensory inputs had an impact on the sensitivity of OSNs. MOR23 neurons under different conditions (closed, untreated, and open) were stimulated by lyral at different concentrations (0.01 or 0.1, 1, 10 and 100 μM) with an

interval > 1 min to minimize odorant adaptation (Fig. 1B–D). For each cell, the peak current induced by each concentration was normalized to the maximum peak current induced by 100 μM lyral. A single dose response curve was then fit based on the data from all neurons under each condition, using a modified Hill equation, $I_{norm} = (I - I_{baseline})/I_{max} = 1 / (1 + (K_{1/2}/C)^n$, where I represents the peak current, $I_{baseline}$ the nonzero mechanical response induced by a Ringer puff (Grosmaitre et al., 2007), I_{max} the maximum current induced by the saturating concentration, $K_{1/2}$ the concentration at which half of the maximum response was reached, C the concentration of lyral, and n the Hill coefficient. Consistent with our previous reports (Grosmaitre et al., 2006; Lee et al., 2011), the dose response curve of MOR23 neurons usually covers four log units from threshold to saturation. The estimated $K_{1/2}$ value decreased from 1.4 μM (n = 17) in the untreated group to 0.6 μM (n = 9) in the closed side, indicating that sensory deprivation increased the sensitivity of MOR23 neurons (Fig. 1E, F). Note that some MOR23 neurons in the closed side responded to lyral at the concentration as low as 0.01 μM (Fig. 1B). An opposite change was observed in the open side, where $K_{1/2}$ value increased to 5.3 μM (n = 10), indicating overexposure decreased the sensitivity of OSNs (Fig. 1E, F).

We next assessed the effect of sensory inputs on adaptation in MOR23 neurons induced by paired lyral pulses with an interval of 10 sec, which usually allowed the first response to return to the baseline (Fig. 2). We analyzed the data at three concentrations (1, 10 and 100 μM) and under three sensory input conditions: closed (Fig. 2A), untreated (Fig. 2B), and open (Fig. 2C). Lower concentrations of lyral at 0.01 or 0.1 μM did not induce odorant responses that can be reliably quantified, and therefore were not included in this analysis. The ratio of the second to the first peak current ($2^{nd}/1^{st}$ *ratio*) was measured for each trial and averaged for each concentration under each condition (Fig. 2D). Two-way ANOVA tests indicated that the $2^{nd}/1^{st}$ ratio of peak currents decreased significantly with increased concentrations but was not affected by the sensory input condition (closed, untreated or open) with the current protocol (Fig.2D and Fig. 3D).

Finally, we investigated the response kinetics of MOR23 neurons under three sensory input conditions: closed, untreated, and open side. The rise time, decay time, and residual current were measured for each trial and averaged for each concentration under each condition (Fig. 1A and Fig. 3). As expected, two-way ANOVA tests showed that the rise time shortened with the increasing concentration ($p = 0.044$) and the decay phase prolonged with the increasing concentration, measured by both the decay time ($p = 0.002$) and normalized residual current $I_{residual}/I_{peak}$ ($p = 4.9E\text{-}5$) (Fig. 3A–D). While the rise time did not depend on the sensory input condition (p = 0.206), the decay phase showed significant dependence (Fig. 3A–D). Sensory deprivation prolonged the decay phase in the closed side compared with the other two conditions ($p = 2.9E\text{-}9$ for the decay time and $p = 0.002$ for $I_{residual}/I_{peak}$, Fig. 3B–D). In summary, sensory experience modulates the sensitivity and response kinetics of MOR23 neurons.

Sensory experience modulates response properties of M71 neurons

We next asked the question whether the experience-dependent changes observed in MOR23 neurons are specific to this receptor type and/or its ligand. We therefore extended the analysis to M71 neurons, which were previously characterized (Bozza et al., 2002). Similarly, M71-IRES-tauGFP mice underwent unilateral naris closure at P3, and M71 neurons from the closed and open nostril were recorded four weeks later with age-matched untreated mice as control. Under voltage clamp mode, brief pulses of acetophenone elicited inward currents in M71 neurons (Fig. 4). We measured the rise time, decay time, and peak currents induced by acetophenone at different concentrations (0.1, 1, 10, and 100 μM) and under each of the three conditions: closed, untreated, and open (Fig. 4A–C). The residual

current was not measured because the responses in M71 neurons usually returned to baseline within 10 sec.

Compared with MOR23 neurons, M71 neurons showed both similar and distinct response properties as well as experience-dependent changes. First, M71 neurons had a much narrower dose response range, which covers 1 to 2 log units from threshold (> 1 μM) to saturation (10 to 100 μM) (Bozza et al., 2002). The narrow dynamic range made it difficult to reliably fit the dose response curves; therefore, we did not determine experience-induced changes in the sensitivity of M71 neurons.

Second, M71 neurons showed similar adaptation induced by paired acetophenone pulses with an interval of 10 sec (Fig. 4A–C). Consistent with the finding in MOR23 neurons, two-way ANOVA tests indicated that the $2^{nd}/1^{st}$ ratio of peak currents decreased significantly with increasing concentrations but was not affected by the sensory input condition (closed, untreated or open) (Fig. 4E).

Third, the response kinetics of M71 neurons was much faster compared with MOR23 neurons. For instance, when stimulated by near-saturating concentration (100 μM) of odorants, the elicited transduction currents in M71 neurons displayed significantly shorter rise time and decay time than MOR23 neurons (rise time: 0.18 ± 0.01 sec, n = 19 for M71 neurons vs 0.30 ± 0.05 sec, n = 44 for MOR23 neurons, $p = 0.022$ in *t* test; decay time: 1.25 ± 0.21 sec for M71 neurons vs 3.03 ± 0.38 sec for MOR23 neurons, $p = 1.2E\text{-}4$ in *t* test). Similar to the analysis performed for MOR23 neurons, we compared the response kinetics of M71 neurons under different conditions (closed, untreated, and open) and at different concentrations (10 and 100 μM) using two-way ANOVA tests. Unlike MOR23 neurons, the rise and decay time of M71 neurons did not differ when stimulated by 10 or 100 μM, but the rise time was significantly shortened in the open side compared with the closed and untreated side (Fig. 4D, E). Despite the differences in the response kinetics between MOR23 and M71 neurons, sensory deprivation prolonged the decay phase of M71 neurons in the closed side as compared with the other two conditions (p = 4.7E-5) (Fig. 4E), consistent with the finding in MOR23 neurons. Therefore, sensory experience in early life modulates the response kinetics of OSNs and the most consistent change is observed in the decay phase, which is slowed down by sensory deprivation.

Sensory deprivation upregulates expression levels of several signaling proteins

The response kinetics of OSNs is likely shaped by many proteins involved in signal transduction. In addition to the key components (ORs, Golf and ACIII) that lead to channel opening, a number of proteins have been shown to influence the response properties of OSNs, including phosphodiesterases (PDE1C and PDE4A) which remove cAMP (Cygnar & Zhao, 2009), β-arrestin-2 which internalizes OR proteins (Mashukova et al., 2006), Ca-calmodulin which mediates inactivation of the CNG channel (Song et al., 2008), and OMP (Buiakova et al., 1996; Ivic et al., 2000; Reisert et al., 2007; Kwon et al., 2009; Lee et al., 2011). The expression levels of these signaling proteins have been studied in unilaterally naris-closed animals (Waguespack *et al.*, 2005; Coppola *et al.*, 2006; Coppola & Waggener, 2012). However, the results obtained from different methods are not always consistent. For example, the mRNA level of G_{olf} was found significantly higher in the closed side as compared with the open side in microarray analysis, but it was not confirmed by quantitative PCR (Coppola & Waggener, 2012) or immunostaining (Coppola *et al.*, 2006). In addition, the effects of naris closure on the olfactory system depend on the laboratory environment in which the animals are kept (Oliva *et al.*, 2010). It is therefore necessary to examine the expression levels of these signaling proteins under our experimental conditions. Using western blot, we compared the expression level of six signaling proteins in the olfactory epithelium between the closed and open side after four-week, unilateral naris closure (Fig.

5). Three proteins (ACIII, PDE4A, and Golf) showed significantly higher expression level in the closed side than in the open side, while three proteins (β-arrestin-2, calmodulin, and PDE1C) showed comparable expression level between the two sides. We then confirmed the results using fluorescent immunostaining (Fig. 6). Coronal sections from three different animals were used and adjacent sections from a single animal were stained by different antibodies. Similar staining patterns were observed from all three animals tested. The olfactory epithelium in the open side was thickened as previously reported (Brunjes, 1994) and the thickening was more evident in the dorsal region (c.f. Fig. 6E and 6E') than in the ventral region (Fig. 6B–D). To facilitate the comparison between the closed and open side, individual images were taken to cover olfactory epithelia on both sides crossing the nasal septum (Fig. 6B–D) or from equivalent regions on the two sides (Fig. 6E). Consistent with the previous reports (Waguespack *et al.*, 2005; Coppola *et al.*, 2006; Coppola & Waggener, 2012) and western blotting, we confirmed that the expression levels of OMP, PDE4A, and ACIII were much higher in the closed side than in the open side (Fig. 6A–C). G_{olf} showed significantly higher staining in some areas (c.f. Fig. 6E and 6E'), but not in others, which may explain why upregulation of G_{olf} in the closed side was not robust in previous reports. The staining level of calmodulin (Fig. 6D) or β-arrestin 2 (not shown) was comparable between the two sides. Interestingly, none of the signaling proteins tested showed higher expression level in the open side compared with the closed side. These experiments indicate that sensory deprivation differentially regulates the expression levels of different signaling proteins, which may play different roles in shaping the response properties (see Discussion).

Discussion

Using patch-clamp recordings, we examined the effects of unilateral naris closure on the functional properties of genetically tagged OSNs with defined ORs. We found that sensory deprivation increased the sensitivity of MOR23 neurons in the closed side while overexposure caused the opposite effect in the open side. The most obvious change in response kinetics is that both MOR23 and M71 neurons in the closed side show prolonged decay phase in odorant-induced transduction events. Using western blotting and antibody staining, we confirmed upregulation of several signaling proteins in the closed side as compared with the open side. This study suggests that early experience modulates response properties of OSNs, probably via modifying the signal transduction cascade.

Here we measured odorant-induced transduction currents from two distinct subtypes of OSNs: MOR23 and M71 neurons. Even though there are individual variations within each subtype (Bozza *et al.*, 2002; Grosmaitre *et al.*, 2006), we demonstrate that some response properties of OSNs depend on OR and/or ligand. The dose-response relationship and response kinetics are distinct for each OR-ligand pair. From threshold to saturation, lyral concentration spans 1000 to 10,000 fold for MOR23 neurons while acetophenone concentration spans only 10 to 100 fold for M71 neurons. Additionally, the transduction currents induced by lyral in MOR23 neurons are much slower than those induced by acetophenone in M71 neurons (c.f. Fig. 1 and Fig. 4). These differences are potentially caused by several mechanisms. First, they may result from distinct features in OR activation by ligand binding. It is unlikely that the signal transduction cascade is different in OSNs expressing different ORs. It should be noted that the observed response properties may be specific for the tested OR-ligand pair. It is possible that a different ligand would elicit responses with different dose-response relationship and kinetics. Second, they may result from different diffusion and removal processes of different ligands. Although MOR23 and M71 neurons are likely situated in similar microenvironment, we can not rule out that lyral and acetophenone are presented to and removed from the cells differently in the mucus which contains complex components including several odorant binding proteins (Tegoni et

al., 2000; Pelosi, 2001). The observed response properties of MOR23 and M71 neurons may reflect both odorant-OR interaction and peri-receptor events.

The broad dose-response curve of MOR23 neurons makes it practical to assess the effects of unilateral naris closure on the sensitivity of these neurons. Compared with the control, MOR23 neurons in the closed side become more sensitive while those in the open side become less sensitive to lyral (Fig. 1), suggesting that both sensory deprivation and overexposure influence the functionality of OSNs.

Despite the differences in response kinetics displayed by MOR23 and M71 neurons, the decay phase in both cell types is prolonged in the closed side compared with the open side and untreated control (Figs. 2, 4). This is consistent with a previous study using electroolfactogram (EOG) recording, which reveals significant slower recovery kinetics of odorant induced responses in the closed side (Waggener & Coppola, 2007). On the other hand, naris-closure induced changes in the rise time are different for MOR23 and M71 neurons. This could be due to actual differences in the OR activation process or methodological factors. The rise time is relatively short and the exact start point of a response sometimes has to be estimated, which makes measurement of the rise time less accurate than that of the decay time. Recordings from more subtypes of OSNs will help to differentiate these possibilities.

There are some differences between our patch clamp data and the previous EOG study by Waggener and Coppola (2007). Our study indicates that the differences between the closed and open side are evident for all concentrations tested, while they report no difference at highest concentration. In addition, our study reveals significant differences between the open side and the untreated control in response sensitivity (Fig. 1) and kinetics (Figs. 3, 4), which are not observed in the EOG study. Such discrepancy could be due to the differences in the recording methods, which assess different response parameters. While patch clamp recording measures transduction currents from individual OSNs, EOG summates signals from many OSNs expressing different ORs, which may dilute the differences present in a subset of OSNs. In fact, the open side is significantly different from the untreated control in morphology and gene/protein expression profile (Coppola *et al.*, 2006; Tian & Ma, 2008; Coppola & Waggener, 2012). In unilaterally naris-closed animals, the open side represents a condition of overstimulation, because of the increased airflow (thus more odorant influx) and lack of the resting periods under normal conditions.

Many signaling proteins are potentially involved in shaping the decay phase of odorant-induced transduction currents. To understand the molecular and cellular mechanisms underlying the observed changes induced by sensory experience, we analyzed the expression levels of several proteins by western blotting and antibody staining. Consistent with previous reports (Waguespack *et al.*, 2005; Coppola *et al.*, 2006; Coppola & Waggener, 2012), we confirmed upregulation of OMP, PDE4A, ACIII and G_{olf} in the closed side (Figs. 5, 6). Interestingly, knocking out OMP has been shown to prolong the decay phase of odorant-induced responses (Buiakova et al., 1996; Ivic et al., 2000; Reisert et al., 2007; Kwon et al., 2009; Lee et al., 2011), which represents the most significant delay in recovery kinetics reported in the literature. With elevated OMP level, OSNs in the closed side also display slowed decay phase, suggesting that the OMP level per se is not sufficient to define the recovery kinetics.

Curiously, the expression level of PDE4A and ACIII is upregulated in two opposite scenarios concerning the OMP level: in the closed side with elevated OMP and in OMP null mice (Lee et al., 2011). Odorant-induced phosphorylation of ACIII has been proposed to contribute to termination of odorant responses (Wei et al., 1998). It would be interesting to

determine whether sensory deprivation can compromise this process and thus slow down the recovery. The role of PDE4A, which is located throughout OSNs except the cilia, in shaping the response kinetics is elusive. Genetic ablation of PDE4A alone does not cause significant changes in response kinetics, but knocking out both PDE1C (which is located in the cilia) and PDE4A prolongs the decay phase (Cygnar & Zhao, 2009). If PDE4A plays any role in signal transduction, the elevated level in the closed side should help to remove cAMP and terminate the response sooner. Therefore the altered PDE4A level is most likely compensating for other changes that cause delay in response recovery.

It is still not clear how unilateral naris closure influences the expression level of OR proteins, the primary detectors of odor molecules. Using in situ hybridization which detects mRNA levels for individual ORs, we recently found that OSNs in the dorsal zone where both MOR23 and M71 neurons reside show lower levels of OR gene expression in the closed side (unpublished data). It is possible that sensory deprivation causes a downregulation of OR proteins, which in turn induce upregulation of the signaling proteins to compensate for the functional loss (Waggener & Coppola, 2007). Consistent with this idea, among all the signaling proteins we tested by immunostaining, the expression level in the closed side is either elevated or similar to that in the open side without any exception. The current study reveals that sensory deprivation causes differential changes in multiple signaling proteins, which may underlie the functional modifications of OSNs.

Acknowledgments

This work was supported by the National Institute on Deafness and Other Communication Disorders, National Institute of Health. The authors declare no conflict of interests.

Abbreviations

OSN	Olfactory Sensory Neuron
OR	Odorant Receptor
GFP	Green Fluorescent Protein
G_{olf}	Olfactory G Protein
ACIII	Adenylyl Cyclase type III
CNG	Cyclic Nucleotide Gated
PDE	Phosphodiesterase
OMP	Olfactory Marker Protein
NCAM	Neural Cell Adhesion Molecule

References

Bennett MK, Kulaga HM, Reed RR. Odor-evoked gene regulation and visualization in olfactory receptor neurons. Mol Cell Neurosci. 2010; 43:353–362. [PubMed: 20080187]

Benson TE, Ryugo DK, Hinds JW. Effects of sensory deprivation on the developing mouse olfactory system: a light and electron microscopic, morphometric analysis. J Neurosci. 1984; 4:638–653. [PubMed: 6707729]

Bozza T, Feinstein P, Zheng C, Mombaerts P. Odorant receptor expression defines functional units in the mouse olfactory system. J Neurosci. 2002; 22:3033–3043. [PubMed: 11943806]

Brunjes PC. Unilateral odor deprivation: time course of changes in laminar volume. Brain Res Bull. 1985; 14:233–237. [PubMed: 3995366]

Brunjes PC. Unilateral naris closure and olfactory system development. Brain Res Brain Res Rev. 1994; 19:146–160. [PubMed: 8167658]

Buiakova OI, Baker H, Scott JW, Farbman A, Kream R, Grillo M, Franzen L, Richman M, Davis LM, Abbondanzo S, Stewart CL, Margolis FL. Olfactory marker protein (OMP) gene deletion causes altered physiological activity of olfactory sensory neurons. Proc Natl Acad Sci U S A. 1996; 93:9858–9863. [PubMed: 8790421]

Coppola DM, Waggener CT. The Effects of Unilateral Naris Occlusion on Gene Expression Profiles in Mouse Olfactory Mucosa. J Mol Neurosci. 2012 In Press.

Coppola DM, Waguespack AM, Reems MR, Butman ML, Cherry JA. Naris occlusion alters transductory protein immunoreactivity in olfactory epithelium. Histol Histopathol. 2006; 21:487–501. [PubMed: 16493579]

Cummings DM, Belluscio L. Continuous neural plasticity in the olfactory intrabulbar circuitry. J Neurosci. 2010; 30:9172–9180. [PubMed: 20610751]

Cummings DM, Brunjes PC. Changes in cell proliferation in the developing olfactory epithelium following neonatal unilateral naris occlusion. Experimental Neurology. 1994; 128:124–128. [PubMed: 8070515]

Cygnar KD, Zhao H. Phosphodiesterase 1C is dispensable for rapid response termination of olfactory sensory neurons. Nat Neurosci. 2009; 12:454–462. [PubMed: 19305400]

Farbman AI, Brunjes PC, Rentfro L, Michas J, Ritz S. The effect of unilateral naris occlusion on cell dynamics in the developing rat olfactory epithelium. Journal of Neuroscience. 1988; 8:3290–3295. [PubMed: 2459323]

Franks KM, Isaacson JS. Synapse-specific downregulation of NMDA receptors by early experience: a critical period for plasticity of sensory input to olfactory cortex. Neuron. 2005; 47:101–114. [PubMed: 15996551]

Gomez-Pinilla F, Guthrie KM, Leon M, Nieto-Sampedro M. NGF receptor increase in the olfactory bulb of the rat after early odor deprivation. Brain Res Dev Brain Res. 1989; 48:161–165.

Grosmaitre X, Santarelli LC, Tan J, Luo M, Ma M. Dual functions of mammalian olfactory sensory neurons as odor detectors and mechanical sensors. Nat Neurosci. 2007; 10:348–354. [PubMed: 17310245]

Grosmaitre X, Vassalli A, Mombaerts P, Shepherd GM, Ma M. Odorant responses of olfactory sensory neurons expressing the odorant receptor MOR23: a patch clamp analysis in gene-targeted mice. Proc Natl Acad Sci U S A. 2006; 103:1970–1975. [PubMed: 16446455]

Hamilton KA, Coppola DM. Distribution of GluR1 is altered in the olfactory bulb following neonatal naris occlusion. J Neurobiol. 2003; 54:326–336. [PubMed: 12500308]

Ivic L, Pyrski MM, Margolis JW, Richards LJ, Firestein S, Margolis FL. Adenoviral vector-mediated rescue of the OMP-null phenotype in vivo. Nat Neurosci. 2000; 3:1113–1120. [PubMed: 11036268]

Kim HH, Puche AC, Margolis FL. Odorant deprivation reversibly modulates transsynaptic changes in the NR2B-mediated CREB pathway in mouse piriform cortex. J Neurosci. 2006; 26:9548–9559. [PubMed: 16971539]

Kosaka T, Kosaka K, Hama K, Wu JY, Nagatsu I. Differential effect of functional olfactory deprivation on the GABAergic and catecholaminergic traits in the rat main olfactory bulb. Brain Res. 1987; 413:197–203. [PubMed: 2885074]

Kwon HJ, Koo JH, Zufall F, Leinders-Zufall T, Margolis FL. Ca extrusion by NCX is compromised in olfactory sensory neurons of OMP mice. PLoS One. 2009; 4:e4260. [PubMed: 19165324]

Lee AC, He J, Ma M. Olfactory marker protein is critical for functional maturation of olfactory sensory neurons and development of mother preference. J Neurosci. 2011; 31:2974–2982. [PubMed: 21414919]

Liu N, Cigola E, Tinti C, Jin BK, Conti B, Volpe BT, Baker H. Unique regulation of immediate early gene and tyrosine hydroxylase expression in the odor-deprived mouse olfactory bulb. J Biol Chem. 1999; 274:3042–3047. [PubMed: 9915843]

Ma M. Encoding Olfactory Signals via Multiple Chemosensory Systems. Crit Rev Biochem Mol Biol. 2007; 42:463–480. [PubMed: 18066954]

Ma M, Chen WR, Shepherd GM. Electrophysiological characterization of rat and mouse olfactory receptor neurons from an intact epithelial preparation. J Neurosci Methods. 1999; 92:31–40. [PubMed: 10595701]

Ma M, Grosmaitre X, Iwema CL, Baker H, Greer CA, Shepherd GM. Olfactory signal transduction in the mouse septal organ. J Neurosci. 2003; 23:317–324. [PubMed: 12514230]

Mashukova A, Spehr M, Hatt H, Neuhaus EM. Beta-arrestin2-mediated internalization of mammalian odorant receptors. J Neurosci. 2006; 26:9902–9912. [PubMed: 17005854]

Mombaerts P. Axonal wiring in the mouse olfactory system. Annu Rev Cell Dev Biol. 2006; 22:713–737. [PubMed: 17029582]

Oliva AM, Salcedo E, Hellier JL, Ly X, Koka K, Tollin DJ, Restrepo D. Toward a mouse neuroethology in the laboratory environment. PLoS One. 2010; 5:e11359. [PubMed: 20613876]

Pelosi P. The role of perireceptor events in vertebrate olfaction. Cell Mol Life Sci. 2001; 58:503–509. [PubMed: 11361085]

Philpot BD, Foster TC, Brunjes PC. Mitral/tufted cell activity is attenuated and becomes uncoupled from respiration following naris closure. J Neurobiol. 1997; 33:374–386. [PubMed: 9322155]

Reisert J, Yau KW, Margolis FL. Olfactory marker protein modulates the cAMP kinetics of the odour-induced response in cilia of mouse olfactory receptor neurons. J Physiol. 2007; 585:731–740. [PubMed: 17932148]

Song Y, Cygnar KD, Sagdullaev B, Valley M, Hirsh S, Stephan A, Reisert J, Zhao H. Olfactory CNG channel desensitization by Ca2+/CaM via the B1b subunit affects response termination but not sensitivity to recurring stimulation. Neuron. 2008; 58:374–386. [PubMed: 18466748]

Su CY, Menuz K, Carlson JR. Olfactory perception: receptors, cells, and circuits. Cell. 2009; 139:45–59. [PubMed: 19804753]

Suh KS, Kim SY, Bae YC, Ronnett GV, Moon C. Effects of unilateral naris occlusion on the olfactory epithelium of adult mice. Neuroreport. 2006; 17:1139–1142. [PubMed: 16837842]

Tegoni M, Pelosi P, Vincent F, Spinelli S, Campanacci V, Grolli S, Ramoni R, Cambillau C. Mammalian odorant binding proteins. Biochim Biophys Acta. 2000; 1482:229–240. [PubMed: 11058764]

Tian H, Ma M. Activity plays a role in eliminating olfactory sensory neurons expressing multiple odorant receptors in the mouse septal organ. Mol Cell Neurosci. 2008; 38:484–488. [PubMed: 18538580]

Touhara K, Vosshall LB. Sensing odorants and pheromones with chemosensory receptors. Annu Rev Physiol. 2009; 71:307–332. [PubMed: 19575682]

Vassalli A, Rothman A, Feinstein P, Zapotocky M, Mombaerts P. Minigenes impart odorant receptor-specific axon guidance in the olfactory bulb. Neuron. 2002; 35:681–696. [PubMed: 12194868]

Waggener CT, Coppola DM. Naris occlusion alters the electro-olfactogram: evidence for compensatory plasticity in the olfactory system. Neurosci Lett. 2007; 427:112–116. [PubMed: 17931777]

Waguespack AM, Reems MR, Butman ML, Cherry JA, Coppola DM. Naris occlusion alters olfactory marker protein immunoreactivity in olfactory epithelium. Brain Res. 2005; 1044:1–7. [PubMed: 15862783]

Wei J, Zhao AZ, Chan GC, Baker LP, Impey S, Beavo JA, Storm DR. Phosphorylation and inhibition of olfactory adenylyl cyclase by CaM kinase II in Neurons: a mechanism for attenuation of olfactory signals. Neuron. 1998; 21:495–504. [PubMed: 9768837]

Zhang X, Zhang X, Firestein S. Comparative genomics of odorant and pheromone receptor genes in rodents. Genomics. 2007; 89:441–450. [PubMed: 17303377]

Zou DJ, Feinstein P, Rivers AL, Mathews GA, Kim A, Greer CA, Mombaerts P, Firestein S. Postnatal refinement of peripheral olfactory projections. Science. 2004; 304:1976–1979. [PubMed: 15178749]

Zufall F, Leinders-Zufall T. The cellular and molecular basis of odor adaptation. Chem Senses. 2000; 25:473–481. [PubMed: 10944513]

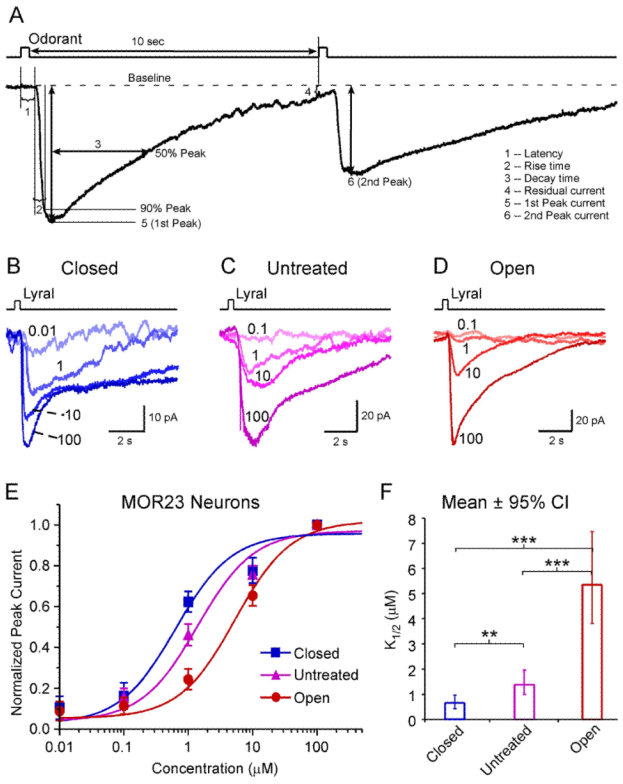

Figure 1.

The sensitivity of MOR23 neurons is increased in the closed side but decreased in the open side. (A) Analysis of transduction currents induced by a pair of odorant pulses under voltage-clamp mode. The latency (1) is the time between the onset of the stimulus and the starting point of the response. The rise time (2) is the time it takes for the current to reach 90% of the peak from the starting point of the response. The decay time (3) is the time it takes for the current to return to 50% of the peak from the peak. The “residual” current (4) is measured 10 sec after the stimulation. The peak currents (5, 6) are induced by the first and second pulse, respectively. (B–D) Inward currents were elicited by lyral pulses at varying concentrations (in μM) under different conditions: closed (n = 9 cells from 8 animals), untreated (n = 17 cells from 9 animals), and open (n = 10 cells from 4 animals). The traces in each panel were from a single neuron. The holding potential was −65 mV for all neurons. (E) The dose-response curves are plotted for different conditions. (F) The $K_{1/2}$ value is summarized for different conditions. Bonferroni multiple comparisons were performed for log$K_{1/2}$ among the three groups (*** marks p <0.001 and ** marks p < 0.01): p = 4.1E–14 (closed vs open), p = 1.1E–6 (untreated vs open), and p = 7.2E–3. For easier comprehension, the mean $K_{1/2}$ ± 95% confidence interval (CI) is plotted here.

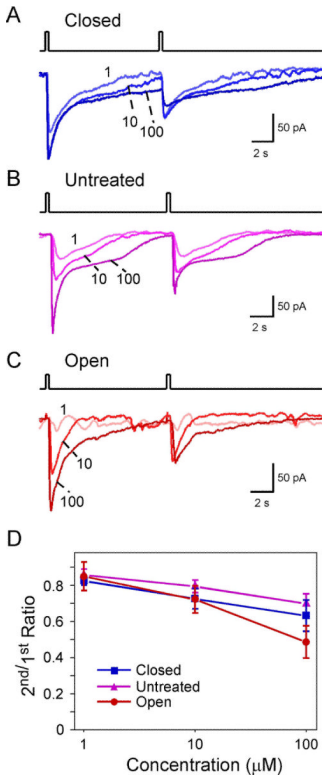

Figure 2.

Adaptation induced by paired pulses depends on the concentration but not on the sensory experience. (A–C) Inward currents were elicited by paired lyral pulses at varying concentrations (in μM) under different conditions: closed (n = 9 cells from 8 animals), untreated (n = 17 cells from 9 animals), and open (n = 10 cells from 4 animals). The traces in each panel were from a single neuron. The holding potential was −65 mV for all neurons. (D) The $2^{nd}/1^{st}$ peak current ratio was plotted against the concentration. This ratio depends on the concentration (p = 3.2E–6) but not on the sensory experience (p = 0.085) in two-way ANOVA tests (see Fig. 3D). The data were from the same set of neurons in Fig. 1.

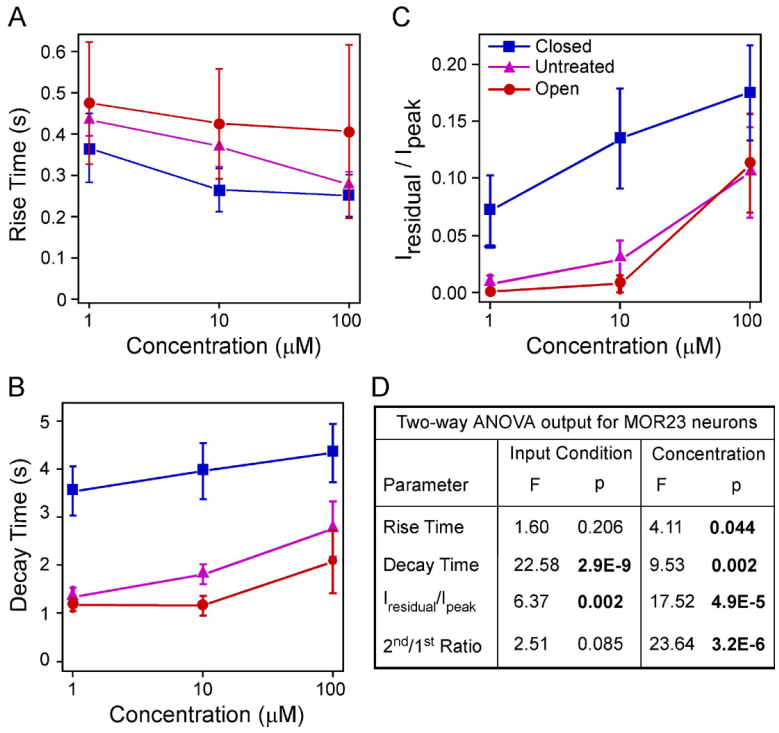

D

Two-way ANOVA output for MOR23 neurons				
	Input Condition		Concentration	
Parameter	F	p	F	p
Rise Time	1.60	0.206	4.11	**0.044**
Decay Time	22.58	**2.9E-9**	9.53	**0.002**
$I_{residual}/I_{peak}$	6.37	**0.002**	17.52	**4.9E-5**
$2^{nd}/1^{st}$ Ratio	2.51	0.085	23.64	**3.2E-6**

Figure 3.

The response kinetics of MOR23 cells depends on sensory experience and concentration. (A–C) Summary of the rise time (A), ratio of the residual current to the peak (B), and decay time (C) under different conditions: closed (n = 9 cells from 8 animals), untreated (n = 17 cells from 9 animals), and open (n = 10 cells from 4 animals). All neurons were recorded under voltage clamp mode with a holding potential of −65 mV. The data were from the same set of neurons in Figs. 1 and 2. (D) Comparison of individual parameters is performed by two-way ANOVA tests based on sensory input condition (coded as a categorical variable) and concentration (coded as an ordinal variable with level 1, 2 and 3 corresponding to 1, 10 and 100 μM, respectively). Significant *p* values are in BOLD. A significant *p* value in input condition indicates difference among the closed, untreated, and open side. A significant *p* value in concentration indicates an increment in concentration increases or decreases the parameter.

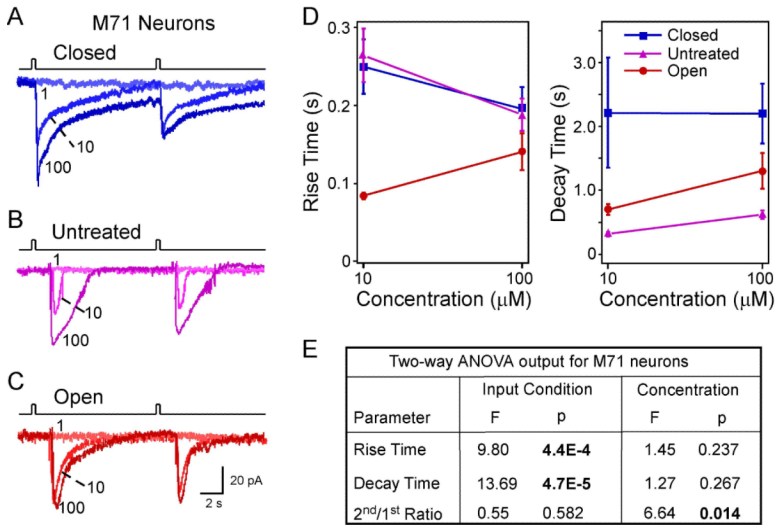

Two-way ANOVA output for M71 neurons				
	Input Condition		Concentration	
Parameter	F	p	F	p
Rise Time	9.80	**4.4E-4**	1.45	0.237
Decay Time	13.69	**4.7E-5**	1.27	0.267
$2^{nd}/1^{st}$ Ratio	0.55	0.582	6.64	**0.014**

Figure 4.

The response kinetics of M71 cells depends on sensory experience and concentration. (A–C) Inward currents were elicited by acetophenone pulses at varying concentrations (in μM) under different conditions: closed (n = 5 cells from 3 animals), untreated (n = 8 cells from 5 animals), and open (n = 6 cells from 3 animals). The traces in each panel were from a single neuron. The holding potential was −65 mV for all neurons. (D) Summary of the rise and decay time under different conditions: closed, untreated, and open. Only two concentrations (10 and 100 μM) were plotted because 1 μM did not elicit measurable responses. (E) Comparison of individual parameters is performed by two-way ANOVA tests based on sensory input condition (coded as a categorical variable) and concentration (coded as an ordinal variable with level 1, 2 and 3 corresponding to 1, 10 and 100 μM, respectively). Significant *p* values are in BOLD.

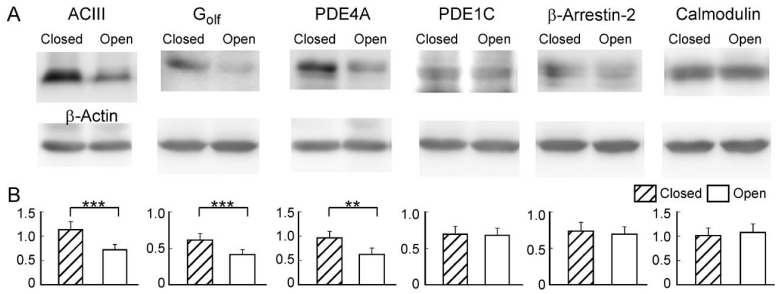

Figure 5.

Sensory experience modulates expression levels of signaling proteins revealed by western blotting. (A) Protein bands were detected by specific antibodies with β-actin serving as control from each sample. (B) Summary of the signaling protein level normalized to that of β-actin. Paired t-test is used to examine the statistical difference between the closed and open side (n = 7 animals) with ** marking $p < 0.01$ and *** marking $p < 0.001$ ($p = 5E–4$ for ACIII; $p = 2E–4$ for G_{olf}; $p = 0.0021$ for PDE4A; $p = 0.83$ for PDE1C; $p = 0.45$ for β-arrestin-2; and $p = 0.44$ for calmodulin).

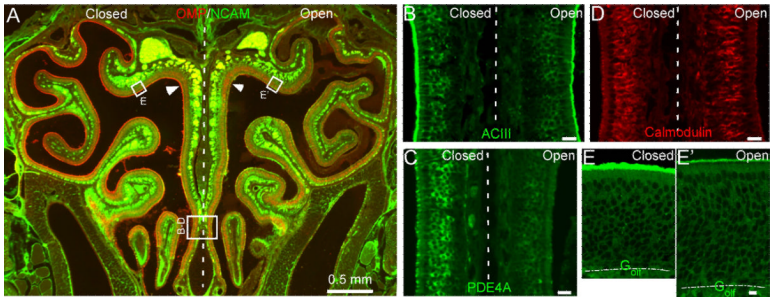

Figure 6.

Sensory experience modulates expression levels of signaling proteins revealed by antibody staining. (A) A coronal section from a four-week-old mouse which underwent neonatal, unilateral naris closure was stained by antibodies against OMP and NCAM. The rectangles in indicate the approximate locations where confocal images (z = 1 μm) in B to E were taken. Arrow heads mark the cilia layer. The vertical dashed line separates the closed (left) and open (right) side. (B–E) Coronal sections were stained by antibodies against ACIII (B), PDE4A (C), calmodulin (D) or G_{olf} (E and E'). Scale bars = 20 μm. Dotted lines in E and E' mark the border between the olfactory epithelium and lamina propria. Note the thicker olfactory epithelium in the open side than in the closed side.